Binding and Reduction of Silver Ions in Thin Polymeric Films of poly-[Fe(vbpy)2(CN)2],poly-vbpy

ARTICLE *in* INORGANIC CHEMISTRY · AUGUST 1994

Impact Factor: 4.76 · DOI: 10.1021/ic00096a019

5 AUTHORS, INCLUDING:

Mohammed Bakir
The University of the West Indies at Mona

103 PUBLICATIONS **1,003** CITATIONS

SEE PROFILE

Binding and Reduction of Silver Ions in Thin Polymeric Films of poly-[Fe(vbpy)$_2$(CN)$_2$],poly-vbpy

Mohammed Bakir,† Susan G. MacKay,§ Richard W. Linton, B. Patrick Sullivan,‡ and Thomas J. Meyer*

Department of Chemistry, University of North Carolina, Chapel Hill, North Carolina 27599-3290

Received December 14, 1993®

Thin films of poly-[Fe(vbpy)$_3$](PF$_6$)$_2$ formed an electrode surfaces by reductive electropolymerization of [Fe(vbpy)$_3$](PF$_6$)$_2$ (vbpy is 4-methyl-4′-vinyl-2,2′-bipyridine) undergo vbpy displacement with [NEt$_4$]CN in acetonitrile to give poly-[Fe(vbpy)$_2$(CN)$_2$],poly-vbpy. The dicyano films incorporate AgNO$_2$ forming poly-[Fe(vbpy)$_2$(CN)(CNAg)](NO$_2$),poly-vbpy as shown by FT-IR and XPS. Electrochemical reduction results in the formation of colloidal silver particles dispersed throughout the films. Under potential hold conditions, further aggregation occurs accompanied by diffusion to the film–electrode interface. Incorporation of AgNO$_2$ into films of poly-[Fe(vbpy)$_3$](PF$_6$)$_2$ also occurs but by partitioning rather than chemical binding. Electrochemical reduction gives colloidal Ag^0. Reduction of either film with AgNO$_2$ in the external solution results in the formation of <0.5 to 2–3 μm sized particles on the film surface as shown by SEM measurements.

Introduction

Development of the chemistry of small domains requires the ability to control both composition and structure in confined volumes. Thin polymeric films of transition metal complexes formed by electropolymerization on conducting substrates offer this control and the versatile chemical and physical properties of the complexes themselves.[1] Combined electrochemical–photochemical procedures are available for creating microstructural features in these films with spatial control.[2]

There is also an exploitable coordination chemistry. In one example, films of poly-[Zn(vbpy)$_3$]$^{2+}$ (vbpy = 4-vinyl-4′-methylbipyridyl) or poly-[Rh(vbpy)(COD)]$^+$ (COD = 1,5-cyclooctadiene) which contain labile metal ions were prepared by reductive electropolymerization.[3] The metal ions could be removed, either by ion exchange or the addition of chelating agents to an external solution. For poly-[Rh(vbpy)(COD)]$^+$, reduction in the presence of CO$_2$ and [Rh(vbpy)(COD)]$^+$ in the external solution gave a catalytic film that contained Rh particles encapsulated in a thin film matrix of poly-vbpy.[4] The films offer the possibility of providing a ligating environment for modifying the properties of other clusters or colloidal particles and confining them within the film matrix.

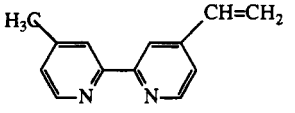

vbpy

In this paper we extend the coordination chemistry of these films to the binding and reduction of Ag(I). Displacement of vbpy from poly-[Fe(vbpy)$_3$](PF$_6$)$_2$[3] by CN$^-$ gives poly-[Fe(vbpy)$_2$(CN)$_2$],poly-vbpy (eq 1) and a basis for Ag(I) binding to either a cyano group or a displaced poly-vbpy. The coordination chemistry of M(bpy)$_2$(CN)$_2$ (M = Fe, Ru, Os) complexes in solution has been documented[6] and includes protonation at cyanide,[6,7] formation of cyano-bridged adducts with Lewis acids[8] and metal ions,[9] and formation of cyano-bridged oligomers.[6,10]

$$\text{poly-[Fe(vbpy)}_3\text{](PF}_6\text{)}_2 + 2\text{CN}^- \rightarrow \text{poly-[Fe(vbpy)}_2\text{(CN)}_2\text{],poly-vbpy} + 2\text{PF}_6^- \quad (1)$$

Experimental Section

Materials. The compound 4-vinyl-4′-methyl-2,2′-bipyridine (vbpy) and the salt [Fe(vbpy)$_3$](PF$_6$)$_2$ were prepared as described in the literature.[5] Tetra-*n*-butylammonium hexafluorophosphate, [N(*n*-Bu)$_4$](PF$_6$), was purchased from Aldrich Chemical Co. Inc., recrystallized

† Present Address: Department of Chemistry, University of the West Indies, Mona, Kingston 7, Jamaica, WI.

‡ Present Address: Department of Chemistry, University of Wyoming, Laramie, WY 82071-3838.

§ Present address: Corporate Research Laboratory 201-25-16, St. Paul, MN 55144.

® Abstract published in *Advance ACS Abstracts,* June 15, 1994.

(1) (a) Calvert, J. M.; Schmehl, R. H.; Sullivan, B. P.; Facci, J. S.; Meyer, T. J.; Murray, R. W. *Inorg. Chem.* **1983**, *22*, 2151. (b) O'Toole, T. R.; Margerum, L. D.; Bruce, M. R.; Sullivan, B. P.; Murray, R. W.; Meyer, T. J. *J. Electroanal. Chem. Interfacial Electrochem.* **1989**, *259*, 217. (c) Deronzier, A.; Moutet, J.-C. *Acc. Chem. Res.* **1989**, *22*, 249. (d) Merz, A. In *Topics in Current Chemistry-Electrochemistry IV*; Springer Verlag: Berlin, Germany, 1990; p 49. (e) Abruña, H. D. *Coord. Chem. Rev.* **1988**, *86*, 135. (f) Murray, R. W. *Annu. Rev. Mater. Sci.* **1984**, *14*, 145.

(2) (a) O'Toole, T. R.; Sullivan, B. P.; Meyer, T. J. *Inorg. Chem.* **1989**, *111*, 5699. (b) Gould, S.; O'Toole, T. R.; Meyer, T. J. *J. Am. Chem. Soc.* **1990**, *112*, 9490. (c) Gray, K. H.; Gould, S.; Leasure, R. M.; Musselman, I. H.; Lee, J.-J.; Meyer, T. J.; Linton, R. W. *J. Vac. Sci. Technol. A* **1992**, *10*, 2679. (d) Gould, S.; Meyer, T. J. *J. Am. Chem. Soc.* **1991**, *113*, 7442. (e) Gould, S.; Gray, K. H.; Linton, R. W.; Meyer, T. J. *Inorg. Chem.* **1992**, *31*, 5521.

(3) Meyer, T. J.; Sullivan, B. P.; Caspar, J. V. *Inorg. Chem.* **1987**, *26*, 4145.

(4) O'Toole, T. R.; Meyer, T. J.; Sullivan, B. P. *Chem. Mater.* **1989**, *1*, 574.

(5) (a) Abruna, H. D.; Denisevich, P.; Umaña, M.; Meyer, T. J.; Murry, R. W. *J. Am. Chem. Soc.* **1981**, *103*, 1. (b) Denisevich, P.; Abruña, H. D.; Leidner, R. C.; Meyer, T. J.; Murray, R. W. *J. Am. Chem. Soc.* **1982**, *21*, 2153.

(6) (a) Hawker, P. N. In *Comprehensive Coordination Chemistry*; Pergamon: Oxford, England, 1987; Vol. 4, Chapter 44. (b) Schroder, M.; Stephenson, T. A. In *Comprehensive Coordination Chemistry*; Pergamon: Oxford, England, 1987; Vol. 4, Chapter 45. (c) Griffith, W. P. In *Comprehensive Coordination Chemistry*; Pergamon: Oxford, England, 1987; Vol. 4, Chapter 46.

(7) (a) Schilt, A. A. *J. Am. Chem. Soc.* **1960**, *82*, 3000. (b) Burgess, J.; Radulovic, S.; Sanchez, F. *Transition Met. Chem.* **1987**, *12*, 536. (c) Bjerrum, J.; Adamson, A. W.; Bostrup, O. *Acta Chem. Scand.* **1956**, *10*, 329. (d) Burgess, J. *J. Chem. Soc., Dalton Trans.* **1972**, 203. (e) Balazani, V.; Carassiti, V.; Moggi, L. *Inorg. Chem.* **1964**, *3*, 1252. (f) Peterson, S. H.; Demas, J. N. *J. Am. Chem. Soc.* **1976**, *98*, 7880. (g) Peterson, S. H.; Demas, J. N. *J. Am. Chem. Soc.* **1979**, *101*, 6576.

(8) Shriver, D. F.; Posner, J. *J. Am. Chem. Soc.* **1966**, *88*, 1672.

(9) (a) Demas, J. N.; Addington, J. W. *J. Am. Chem. Soc.* **1974**, *96*, 3663. (b) Kinnaird, M. G.; Whitten, D. G. *Chem. Phys. Lett.* **1982**, *88*, 275.

(10) (a) Bignozzi, C. A.; Scandola, F. *Inorg. Chem.* **1984**, *23*, 1540. (b) Bignozzi, C. A.; Roffia, C. C.; Davila, M. T. I.; Scandola, F. *Inorg. Chem.* **1989**, *28*, 4358. (c) Bignozzi, C. A.; Roffia, C. C.; Scandola, F. *J. Am. Chem. Soc.* **1985**, *107*, 1644. (d) Bignozzi, C. A.; Paradisi, C.; Roffia, C. C.; Scandola, F. *Inorg. Chem.* **1988**, *27*, 408. (e) Bignozzi, C. A.; Argazzi, R.; Schoonover, J. R.; Gordon, K. C.; Dyer, R. B.; Scandola, F. *Inorg. Chem.* **1992**, *31*, 5260.

0020-1669/94/1333-3945$04.50/0

twice from ethanol/water, and dried under vacuum for 24 h. Tetraethylammonium cyanide, $[NEt_4]CN$, was purchased from Fluka Chemilea, Bucks, Switzerland, and used as received. Solvents were of the highest purity grade quality and were deoxygenated prior to use by a N_2 purge. The salts $AgNO_3$ and $AgNO_2$ were obtained from commercial sources and used as received.

Instrumentation. Electrochemical experiments were performed in CH_3CN solutions that were 0.1 M in $[N(n\text{-}Bu)_4](PF_6)$. The $E_{p,a}$, $E_{p,c}$, and $E_{1/2} = (E_{p,a} + E_{p,c})/2$ values were referenced to the sodium chloride saturated calomel electrode, SSCE, at room temperature and are uncorrected for junction potentials. Voltammetric experiments were performed with the use of a Princeton Applied Research (PAR) Model 173 galvanostat and with either a PAR Model 175 universal programmer or a home built supercycle.[11] Data were recorded on either Soltec or Hewlett-Packard HP-7015B X-Y recorders. Electrochemical cells were of conventional design based on scintillation vials or H-cells. Pt-button, glassy-carbon buttons, planar Pt, indium–tin–oxide (ITO), or Au sputtered on Cr/Si/SiO plates were used as working electrodes. Specular reflectance IR spectra of films cast on either planar Pt or Au electrodes were recorded with the use of a Nicolet 20DX FT-IR spectrometer in conjunction with a variable-angle specular reflectance attachment (Barnes Analytical). Electronic absorption spectra of films cast on tin-doped indium oxide (ITO) optically transparent electrodes were recorded by using an HP-845A spectrophotometer. X-ray photoelectron spectra (XPS) of the films cast on Pt electrodes were obtained by using a Perkin-Elmer Physical Electronics Model 5400 XPS spectrometer equipped with a differentially pumped Ar ion gun. The X-ray source in these studies was Mg k_α radiation (1253.6 eV), with an analysis area of 1.1 mm^2, hemispherical analyzer pass energy of 35.75 eV, and anode power of 400 W (15 kV). Electron micrographs were taken for films cast on Pt electrodes by using an ISI DS-130 scanning electron microscope (SEM) with an accelerating voltage of 6 keV and secondary electron detection.

Film Chemistry of poly-$[Fe(vbpy)_3](PF_6)_2$. Following standard literature procedures,[5] electrodes coated with films of poly-$[Fe(vbpy)_3](PF_6)_2$ were prepared in 0.1 M $[N(n\text{-}Bu)_4](PF_6)/CH_3CN$ solutions containing $[Fe(vbpy)_3](PF_6)_2$ by scanning reductively between 0 and −1.7 V or between −0.7 and −1.7 V (*vs* SSCE). The resulting red films were removed from solution, washed with CH_3CN, and dried under a nitrogen atmosphere. Film coverages, as estimated from integrated peak areas under the wave for the $Fe^{III/II}$ couple, were in the range 1×10^{-7} to 1×10^{-9} mol/cm^2 on 0.125 cm^2 Pt-disk electrodes. The observations made in the study concerning the binding and subsequent reduction of Ag^+ were, at least qualitatively, independent of film thickness.

poly-$[Fe(vbpy)_2(CN)_2]$,poly-vbpy. Films of poly-$[Fe(vbpy)_3](PF_6)_2$ were converted into poly-$[Fe(vbpy)_2(CN)_2]$,poly-vbpy by soaking in CH_3CN solutions that were 0.1 M in $[NEt_4](CN)$ for 1–2 h. The resulting green films were removed from solution, washed with CH_3CN, and dried.

Binding of Ag^+ in poly-$[Fe(vbpy)_2(CN)_2]$,poly-vbpy. Thin films of poly-$[Fe(vbpy)_2(CN)_2]$,poly-vbpy which contained $AgNO_2$ were prepared by soaking films of poly-$[Fe(vbpy)_2(CN)_2]$,poly-vbpy in CH_3CN solutions that were 0.1 M in added salt for 10–15 min. The resulting red films were removed from solution, washed with CH_3CN, and dried.

Incorporation of Ag^+ into poly-$[Fe(vbpy)_3](PF_6)_2$. The salt $AgNO_2$ was incorporated into films of poly-$[Fe(vbpy)_3](PF_6)_2$ by soaking in 0.1 M $AgNO_2/CH_3CN$ solution for 10 min. The resulting films, which retained their red color, were removed from solution, washed with CH_3CN, and dried.

Reduction of Ag^+ in poly-$[Fe(vbpy)_2(CN)_2]$,poly-vbpy or poly-$[Fe(vbpy)_3](PF_6)_2$. Films containing $AgNO_2$ were reduced electrochemically in 0.1 M $[N(n\text{-}Bu)_4](PF_6)/CH_3CN$ solution to Ag^0 either by holding the potential at a fixed value or by repetitive scans between two fixed potentials as described in detail in later sections.

Removal of Ag^+ from Films of poly-$Fe(vbpy)_2(CN)(CNAg)](NO_2)$,-poly-vbpy. Films of poly-$[Fe(vbpy)_2(CN)(CNAg)](NO_2)$,poly-vbpy were soaked in CH_3CN solutions 0.1 M in $NaS_2CN(CH_2Ph)_2$ (Na(dbdtc)) for 1–2 h. The resulting green films were removed from solution, washed with CH_3CN, and dried.

Results

Incorporation of Ag^+ into poly-$[Fe(vbpy)_2(CN)_2]$,poly-vbpy. Treatment of poly-$[Fe(vbpy)_3](PF_6)_2$ with 0.1 M $[NEt_4]CN$ in CH_3CN resulted in rapid displacement of a single vbpy to give poly-$[Fe(vbpy)_2(CN)_2]$,poly-vbpy (eq 1). The reaction was complete on a time scale of minutes as evidenced by the change in film color from red to green. There is no evidence for further displacement of vbpy by CN^- even over extended periods (hours) consistent with the solution chemistry of $[Fe(bpy)_3]^{2+}$. Our experimental evidence is consistent with retention of the released vbpy in the films and complete, or nearly complete, electropolymerization of the three vbpy ligands. As presented below, the evidence for this conclusion is from the quantitative or near-quantitative return of poly-$[Fe(vbpy)_2(CN)_2]$,poly-vbpy to poly-$[Fe(vbpy)_3]^{2+}$ when loss of CN^- is induced by oxidation to Fe^{III}, Ag^+-assisted substitution, or vbpy-based reduction.

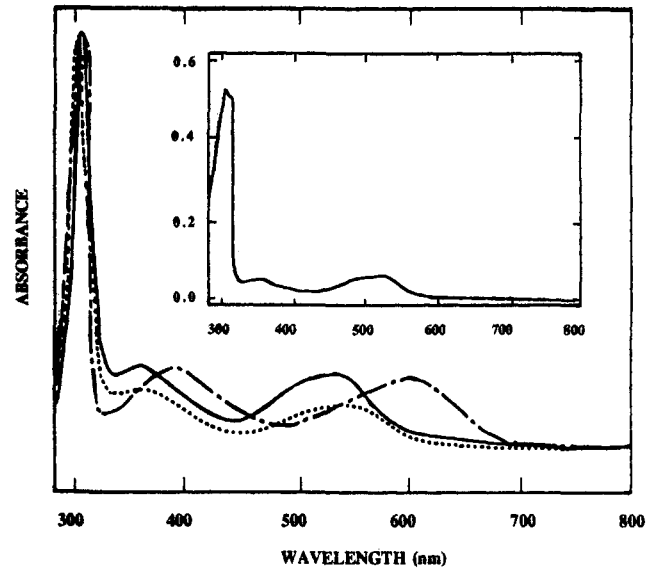

Figure 1. UV–visible spectra of thin films of poly-$[Fe(vbpy)_3](PF_6)_2$ (—), poly-$[Fe(vbpy)_2(CN)_2]$,poly-vbpy (– · –), and poly-$[Fe(vbpy)_2(CN)(CNAg)](NO_2)$,poly-vbpy (···) on planar ITO electrodes. The spectrum of a 5.5×10^{-5} M solution of $Fe(vbpy)_2(CN)_2 \cdot AgNO_2$ in CH_3CN in a 1.0-cm cell is shown in the insert.

Exposure to external solutions containing $AgNO_2$ (0.1 M in CH_3CN) resulted in rapid incorporation of Ag^+ as shown by spectrophotometric measurements on optically transparent ITO electrodes, Figure 1. Incorporation occurred within 10 s for a solution ca. 10^{-3} M in $AgNO_2$.

Evidence for Ag^+ binding, the composition of the films with regard to silver content, and the structural nature of the binding were inferred from the results of a number of experiments. In Figure 2 are shown reflectance FT-IR spectra of three films, poly-$[Fe(vbpy)_3](PF_6)_2$, poly-$[Fe(vbpy)_2(CN)_2]$,poly-vbpy, and poly-$[Fe(vbpy)_2(CN)(CNAg)](NO_2)$,poly-vbpy on Pt substrates. In a comparison of the spectra of poly-$[Fe(vbpy)_3](PF_6)_2$ and poly-$[Fe(vbpy)_2(CN)_2]$,poly-vbpy, the pattern of ν(bpy) ring stretching modes in the region 1350–1650 cm^{-1} is relatively unaffected by the substitution of a vbpy by CN^-. The features of note that do change are the loss of the PF_6^- peak at 842 cm^{-1} and the appearance of a peak at 2080 cm^{-1} and shoulder at 2060 cm^{-1} for the ν(CN) stretching modes. For $Fe(bpy)_2(CN)_2$ in KBr, these bands appear at 2080 and 2074 cm^{-1}.

In a film that had been exposed to 0.1 M $AgNO_2$ in CH_3CN, Figure 2c, significant changes occur in the IR spectrum. These include shifts in the ν(bpy) region and the appearance of a vibration assigned as $\nu(NO_2^-)_{sym}$ at 1217 cm^{-1} due to the incorporation of nitrite as a counterion. In the ν(CN) region new bands appear at 2094 and 2150 cm^{-1} of considerably lessened intensity compared to the 2080-cm^{-1} band in the precursor film. The loss of intensity is consistent with Ag^+ binding to the cyano groups, an effect that has been observed in other cyano-bridged complexes.[8,9b,10a]

In a separate experiment, a comparison of relative ν(CN) peak heights showed that Ag^+ incorporation was complete after 15 min, consistent with the UV–visible measurements. Over longer

(11) Woodward, W. S.; Rocklin, R. D.; Murray, R. W. *Chem. Biomed. Environ. Instrum.* **1979**, *9*, 95.

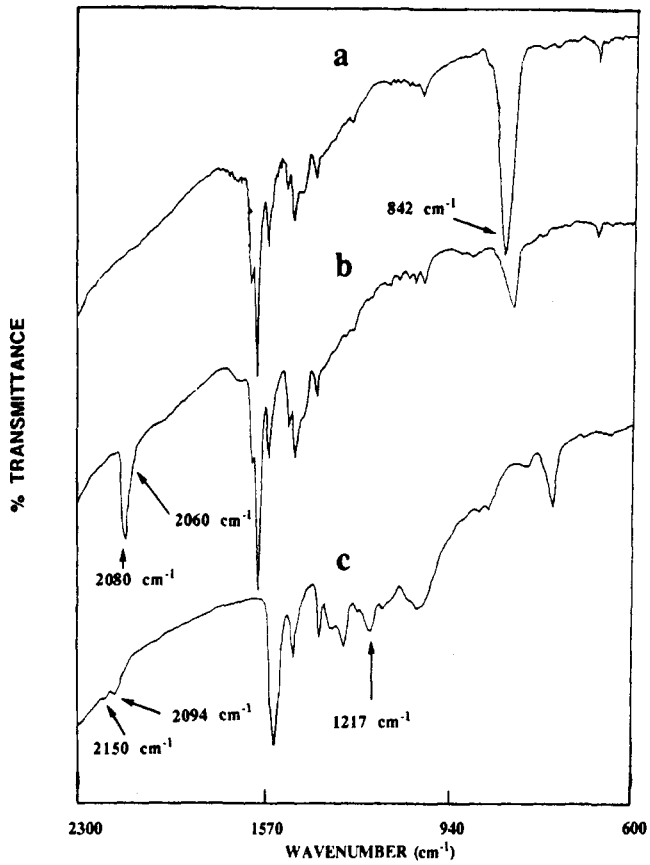

Figure 2. Specular reflectance FT-IR spectra of thin films of (a) poly-[Fe(vbpy)$_3$](PF$_6$)$_2$, (b) poly-[Fe(vbpy)$_2$(CN)$_2$],poly-vbpy, and (c) poly-[Fe(vbpy)$_2$(CN)(CNAg)](NO$_2$),poly-vbpy on planar Pt electrodes.

periods with 1 mM $AgNO_2$ in the external solution, loss of CN^- and re-formation of poly-$[Fe(vbpy)_3]^{2+}$ occurred. In the IR spectrum after 12 h and rinsing with pure CH_3CN, the characteristic ν(CN) and $\nu(NO_2)$ bands were absent and the pattern of ν(bpy) bands for poly-$[Fe(vbpy)_3]^{2+}$ reappeared.

With shorter soaking times (<15 min), the CN^- groups were largely retained as shown by IR measurements. After drying, the films were stable toward CN^- loss for indefinite periods. A set of parallel experiments were conducted with $AgNO_3$. These experiments showed that significant removal of CN^- had occurred even after a soaking period of 15 min.

The changes in UV–visible spectra after incorporation of $AgNO_2$ are consistent with Ag^+ binding to a cyano group, Figure 1. For purposes of comparison, the spectrum of the adduct $[Fe(bpy)_2(CN)(CNAg)]^+$ in CH_3CN is shown as an insert in Figure 1. The sense of the spectral shifts among the three films is consistent with the spectra of related complexes in solution.[7f,g,9b,10a] The visible bands originate from $d\pi(Fe) \rightarrow \pi^*$(bpy) metal-to-ligand charge-transfer (MLCT) transitions. Replacement of poly-vbpy by CN^- causes the shift to lower energy. With binding to Ag^+, the cyano group changes its electronic character and becomes a better π acceptor. This stabilizes $d\pi$, increases the $d\pi \rightarrow \pi^*$ energy gap, and increases the absorption energy.

Elemental composition and distribution of $AgNO_2$ was investigated by XPS, the results of which were described in detail elsewhere.[12] Only results relevant to this study are summarized in Table 1. From these data, the ratio of Ag^+ to Fe^{II} at early soaking times was ~1:1. Spectral deconvolution provided direct evidence for the various N atoms in poly-vbpy, NO_2^-, and CN^-. Data acquired after a soaking period of 15 min demonstrated partial loss of CN^-. The Ag^+/Fe^{II} ratio decreased from 0.95 to 0.90 but remained near 1:1, and the relative intensity of the N atoms of the cyano groups was diminished.

(12) MacKay, S. G.; Bakir, M.; Mussleman, I. H.; Meyer, T. J.; Linton, R. W. *Anal. Chem.* **1991**, *63*, 60.

Table 1. Relative Atomic Concentrations in Films of poly-[Fe(vbpy)$_2$(CN)(CNAg)](NO$_2$),poly-(vbpy)[a]

	atomic ratio					
	N/C					
value	total	vbpy	CN	NO_2	Ag/Fe	Fe/C
measd	0.15	0.11	0.032	0.015	0.95	0.028
theory	0.22	0.15	0.049	0.024	1.00	0.024

[a] $AgNO_2$ was incorporated by soaking the poly-[Fe(vbpy)$_2$(CN)$_2$],poly-(vbpy) film in an acetonitrile solution 0.1 M in $AgNO_2$ for <3 min. The results shown are an average for two films.

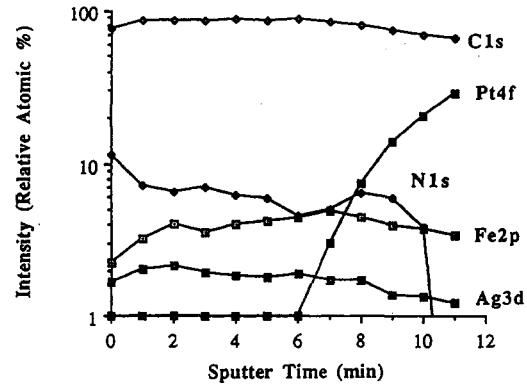

Figure 3. XPS sputter depth profile of a thin film of poly-[Fe(vbpy)$_2$(CN)(CNAg)](NO$_2$),poly-vbpy on a 0.125-cm^2 Pt electrode.

XPS depth profiling experiments were conducted to investigate the spatial distribution of Ag^+. The details were reported elsewhere.[12] In Figure 3 is shown a plot of relative atomic concentration *vs* sputter time. From these data the Ag^+/Fe^{II} ratio remains reasonably constant within the films and Ag^+ is dispersed uniformly.

On the basis of spectroscopic and XPS results, $AgNO_2$ binding in the dicyano films occurs to a single cyano group, eq 2. From the soaking experiments over an extended period, the films are unstable toward Ag^+-assisted loss of CN^- and re-formation of poly-$[Fe(vbpy)_3]^{2+}$, eq 3.

$$\text{poly-[Fe(vbpy)}_2\text{(CN)}_2\text{],poly-vbpy} + AgNO_2 \rightarrow \text{poly-[Fe(vbpy)}_2\text{(CN)(CNAg)](NO}_2\text{),poly-vbpy} \quad (2)$$

$$\text{poly-[Fe(vbpy)}_2\text{(CN)(CNAg)](NO}_2\text{),poly-vbpy} + AgNO_2 \rightarrow \text{poly-[Fe(vbpy)}_3\text{](NO}_2\text{)}_2 + 2AgCN \quad (3)$$

poly-[Fe(vbpy)$_3$](PF$_6$)$_2$·2AgNO$_2$. Films of poly-[Fe(vbpy)$_3$](PF$_6$)$_2$ also incorporate $AgNO_2$. In FT-IR spectra the usual complement of ν(vbpy) bands appears, along with $\nu(NO_2^-)$ at 1217 cm^{-1}. The UV–visible spectrum is relatively unaffected with λ_{max} appearing at 534 nm compared to λ_{max} = 536 nm for $[Fe(bpy)_3]^{2+}$ in CH_3CN. By XPS, a film formed with 0.1 M $AgNO_2$ in the external solution had a Ag^+ to Fe^{II} ratio of ~2:1.

The Ag^+ content of the films depends on the concentration of $AgNO_2$ in the external solution as shown by peak current measurements for the $Ag^{+/0}$ wave; see below. The ratio 2:1 was reached with 0.1 M in $AgNO_2$ suggesting that $AgNO_2$ partitions into these films. With $AgNO_3$ in the external solution at 0.1 M, incorporation was less than 1:1 suggesting a counterion effect. The $AgNO_2$ is entrapped and held within the films allowing electrochemical measurements to be made without significant loss of $AgNO_2$ to the external solution; see below.

Electrochemistry. A cyclic voltammogram of poly-[Fe(vbpy)$_2$(CN)$_2$],poly-vbpy is shown in Figure 4a, in which an $Fe^{III/II}$ wave appears at $E_{1/2}$ = +0.44. For poly-$[Fe(vbpy)_3]^{2+}$ the $Fe^{III/II}$ wave is at $E_{1/2}$ = +1.00 V. In addition, sharp "prewaves" appear at

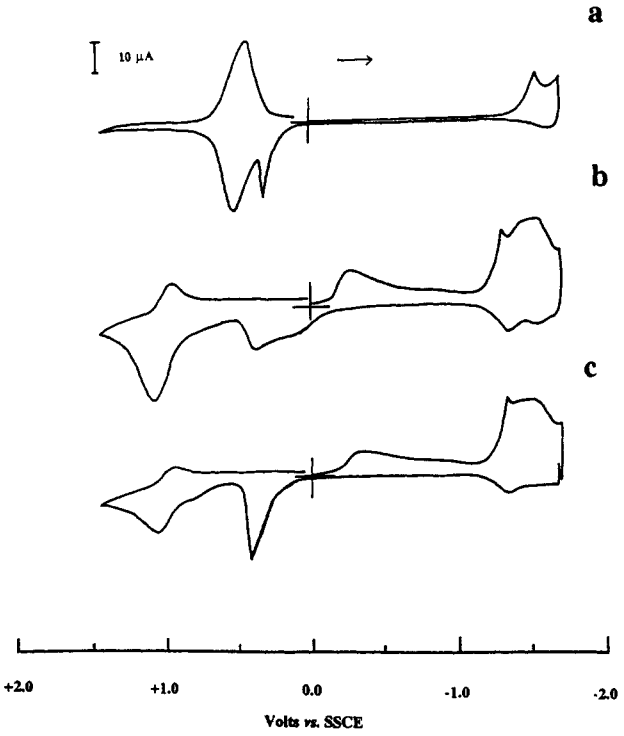

Figure 4. Cyclic voltammograms of thin films on Pt electrodes (0.125 cm^2) in CH_3CN 0.1 M in $[N(n\text{-}Bu)_4)]PF_6$, at a scan rate of 10 mV/s *vs* SSCE: (a) poly-$[Fe(vbpy)_2(CN)_2]$,poly-vbpy; (b) poly-$[Fe(vbpy)_2(CN)(CNAg)](NO_2)$,poly-vbpy, single scan; (c) as in (b) after the potential was scanned to and held at –1.7 V for 1 min.

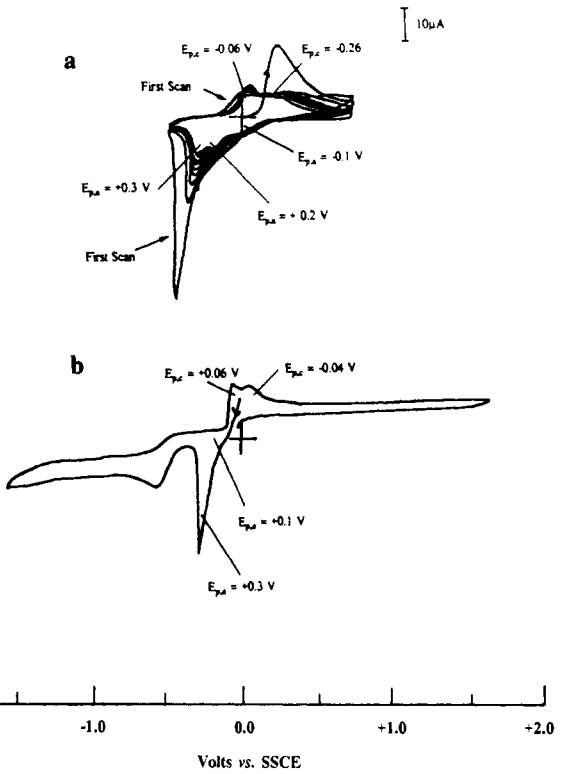

Figure 5. Same as in Figure 4, at a scan rate of 50 mV/s: (a) Repetitive scans between –0.8 and 0.5 V on a film of poly-$[Fe(vbpy)_2(CN)(CNAg)](NO_2)$,poly-vbpy on Pt following a scan to and potential hold at –0.8 V for 2 min; (b) $AgNO_2$ (0.01 M) at a Pt disk electrode (0.125 cm^2).

$E_{p,c} = -1.62$ and $E_{p,a} = +0.31$ V for poly-$[Fe(vbpy)_2(CN)_2]$,-poly-vbpy and at $E_{p,c} = -1.12$ V and $E_{p,a} = +0.88$ V for poly-$[Fe(vbpy)_3]^{2+}$. They appear just before the first vbpy-based or $Fe^{III/II}$ waves and have analogs in related films. They have been attributed to structural changes or trapped sites.[5] For the dicyano films, repetitive scans (≈20) between 0 and +0.80 V resulted in loss of CN^- and formation of poly-$[Fe(vbpy)_3]^{2+}$, either by labilization in oxidation state Fe^{III},

$$\text{poly-}[Fe(vbpy)_2(CN)_2]\text{,poly-vbpy} + 3PF_6^- \xrightarrow{-e^-} \text{poly-}[Fe(vbpy)_3](PF_6)_3 + 2CN^- \quad (4a)$$

or perhaps by oxidation of bound CN^- to cyanogen.

$$\text{poly-}[Fe(vbpy)_2(CN)_2]\text{,poly-bpy} + 2PF_{6^-} \xrightarrow{-2e^-} \text{poly-}[Fe(vbpy)_3](PF_6)_2 + (CN)_2 \quad (4b)$$

In the cyclic voltammogram of poly-$[Fe(vbpy)_2(CN)(CNAg)](NO_2)$,-poly-vbpy in Figure 4b, $E_{1/2}$ for $Fe^{III/II}$ shifts to +1.03 V. Scanning through the Fe^{III}/Fe^{II} wave also gives poly-$[Fe(vbpy)_3]^{2+}$. In poly-$[Fe(vbpy)_3](PF_6)_2$ containing $AgNO_2$, the potential of the $Fe^{III/II}$ couple was +1.00 V. Waves appear in both films from –0.5 to +0.5 V for $Ag^{+/0}$ couples. In either film these waves nearly disappear after scanning past the $Fe^{III/II}$ wave signaling the loss of Ag^+.

In a reductive scan on poly-$[Fe(vbpy)_2(CN)(CNAg)](NO_2)$,-poly-vbpy, a broad Ag^+ reduction wave appeared at $E_{p,c} = -0.26$ V, Figure 4b. It was followed by bpy-based reductions at $E_{1/2} = -1.40$ and $E_{1/2} = -1.55$ V. These waves are shifted positively compared to poly-*cis*-$Fe(vbpy)_2(CN)_2$,poly-bpy where $E_{1/2} = -1.87$ V for the first reduction. Reoxidation of Ag^0 to Ag^+ occurred at $E_{p,a} = +0.12$ and +0.43 V on a reverse scan, and $i_{p,a}$ for the $Fe^{III/II}$ wave at $E_{p,a} = +1.06$ V was enhanced compared to $i_{p,c}$. The shifted bpy waves show that Ag is still interacting with CN^- even after reduction to Ag^0. When the potential was held at –1.7 V for 1 min, the $Ag^{0/+}$ component wave at $E_{p,a} = +0.12$ V was lost with growth of a new wave at $E_{p,a} = +0.43$ V, Figure 4c.

In Figure 5a are illustrated a series of cyclic voltammograms on poly-$[Fe(vbpy)_2(CN)(CNAg)](NO_2)$,poly-vbpy from –0.80 to +0.50 V. In this range, there are no complications from $Fe^{III/II}$ or bpy-based couples. Figure 5a illustrates a reductive scan (showing the usual wave at $E_{p,c} = -0.26$ V) to –0.8 V where the potential was held for 2 min. A series of scans at 50 mV/s was then initiated by scanning in the positive direction. On the first scan after the hold, a wave appeared at $E_{p,a} = +0.43$ V with a reductive component at $E_{p,c} = +0.03$ V. On the second scan the peak current of the oxidative wave had decreased by $\sim 1/2$ and shifted to $E_{p,a} = +0.36$ V. On subsequent scans $i_{p,a}$ continued to decrease and $E_{p,a}$ shifted negatively with $E_{p,c}$ shifting negatively as well. After 12 scans a steady state was reached where there were no further changes in potentials or currents with oxidative waves appearing at $E_{p,a} = +0.3$, +0.2, and –0.1 V and reductive waves at $E_{p,c} = -0.06$ and –0.26 V, Figure 5a. There was little if any loss of Ag under normal cyclic voltammetric scan conditions at 50 mV/s over the same potential range.

A cyclic voltammogram of $AgNO_2$ in 0.1 M $[N(n\text{-}Bu)_4]PF_6/CH_3CN$ is shown in Figure 5b. When the potential was held at 0 V for 1 min, oxidative waves at $E_{p,a} = +0.1$ and +0.3 V and reductive waves at $E_{p,c} = +0.06$ and –0.04 V appeared following an oxidative scan. In addition, an irreversible NO_2^- oxidative wave appeared at $E_{p,a} = +0.53$ V.

Films containing Ag^0 obtained by scanning past the $Ag^{+/0}$ wave at –0.7 V were examined by XPS, Table 2. By using curve resolution techniques,[12] the ratio of oxidation states, Ag^+/Ag^0, was determined to be 1.62 ± 0.50 for the one result cited in Table 2. The appearance of Ag^+ may be a consequence of the single scan with incomplete time for reduction. It could also be artifactual, arising from oxidation of Ag^0 to Ag_2O during transfer from the glovebox to the XPS apparatus. The total Ag/Fe ratio was maintained at close to 1:1 showing that the Ag that was reduced remained in the films.

Table 2. Oxidation State at Ag after Reduction of Poly-[Fe(vbpy)$_2$(CNAg)](NO)$_2$,poly-(vbpy)[a]

component	Ag 3d binding energy (eV)[b]	ratio	
		Ag^+/Ag^0	Ag/Fe^c
Ag^+	368.3 ● 0.2	1.62 ± 0.50	0.88 ± 0.40
Ag^0	367.1 ± 0.1		

[a] After a single reductive scan from 0 to –0.7 V in an acetonitrile solution that was 0.1 M in [N(*n*-Bu)$_4$]PF$_6$ at a scan rate of 5.0 mV/s. [b] The separate binding energies were obtained by curve resolution.[12c] As total Ag (Ag^0 + Ag^+).

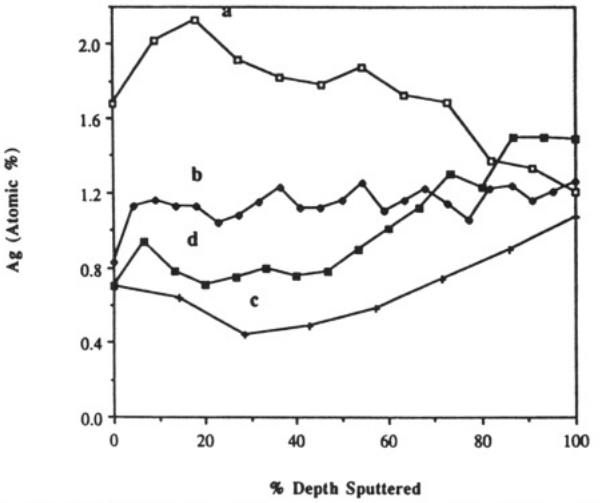

Figure 6. Total Ag (Ag^+ + Ag^0) as a function of depth by XPS sputter depth profiling for thin films on Pt of (a) poly-[Fe(vbpy)$_2$(CN)(CNAg)](NO$_2$),poly-vbpy, (b) poly-[Fe(vbpy)$_2$(CN)(CNAg)](NO$_2$),poly-vbpy after the potential had been held at –0.7 V for 1 min in CH_3CN 0.1 M in [N(n-Bu)$_4$)]PF$_6$, (c) as in (b) after 5 min of reduction at –0.7 V, and (d) as in (b) after reduction at –0.7 V for 15 min.

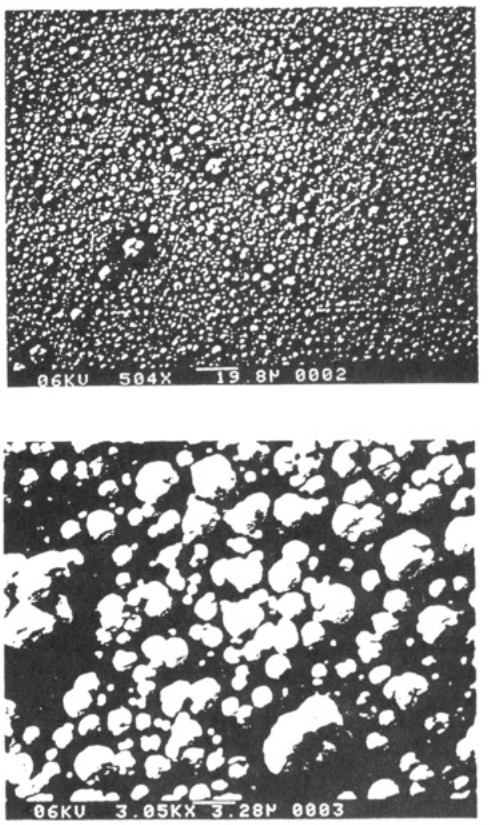

Figure 7. SEM micrographs of silver particles on poly-[Fe(vbpy)$_2$(CN)(CNAg)](NO$_2$),poly-vbpy formed by scanning from 0 to –0.7 V vs SSCE in a 0.1 M [N(*n*-Bu)$_4$)]PF$_6$ solution 0.1 M in $AgNO_2$ at a scan rate of 50 mV/s. The scales for (a) and (b) in μm are indicated at the bottom of the figures.

Spatial distribution was explored by XPS sputter depth profiling, Figure 6. From these data, reduction for 1 min leaves Ag^0 dispersed throughout the film. At longer reduction times (Figure 6c,d), there is a marked skewing of the distribution toward the electrode/film interface.

The electrochemical data provide evidence for different chemical forms of Ag^0 by the varying pattern of $Ag^{+/0}$ couples. On repetitive scans from +0.5 to –0.8 V waves appear at $E_{p,a}$ = +0.43 and $E_{p,c}$ = +0.03 V with the electrode held at –0.8 V for extended periods. On subsequent scans, a sizable fraction of the Ag is lost and, finally, a steady state was reached. At steady state, waves remained at $E_{p,c}$ = –0.06 and –0.26 V and $E_{p,a}$ = –0.10, +0.20, and +0.30 V which were unaffected by further scanning.

Electronic absorption spectra following reduction of poly-[Fe(vbpy)$_2$(CN)(CNAg)](NO$_2$),poly-vbpy at –1.70 V after 1 min showed a new absorption band at λ_{max} = 380 nm. Reduction for 15 min gave λ_{max} = 400 nm.

Electrodeposition of Ag^0. Further Ag^0 could be deposited with $AgNO_2$ in the external solution by repetitive voltammetric scans between 0 and –0.70 V. SEM micrographs at two different resolutions obtained at the end of a scan sequence (10 scans) are shown in Figure 7. Silver particles appear on the surface of the film which are roughly spherical with particle sizes in the range <0.5 to ~3 μm.

Electrochemical Reduction of poly-[Fe(vbpy)$_3$](PF$_6$)$_2$·2AgNO$_2$. Representative cyclic voltammograms of poly-[Fe(vbpy)$_3$](PF$_6$)$_2$·2$AgNO_2$ in CH_3CN are shown in Figure 8. In these voltammograms the $Fe^{III/II}$ and bpy-based couples were relatively unaffected compared to poly-[Fe(vbpy)$_3$](PF$_6$)$_2$ with $E_{1/2}$ values appearing at +1.03, –1.35, and –1.53 V. In Figure 8a is shown the result of a single reductive scan. Reduction of Ag^+ occurred at $E_{p,c}$ = –0.17 V, and oxidation of Ag^0 at $E_{p,a}$ = +0.22 and $E_{p,a}$ = +0.37 V. After a potential hold at –1.7 V for 1 min, a single reoxidation wave appeared at $E_{p,a}$ = +0.42 V (Figure 8b). Following an oxidative scan through the $Fe^{III/II}$ wave at $E_{1/2}$ = +1.03 V, Ag was completely lost from the film.

A series of potential scans from –0.80 and +0.50 V are shown in Figure 8c. An initial wave at $E_{p,c}$ = –0.17 V disappeared with repetitive scanning to be replaced by a waves at $E_{p,a}$ = 0 and +0.2 V and $E_{p,c}$ = –0.04 and $E_{p,c}$ = –0.16 V.

Repetitive scans between 0 and –0.70 V with 0.01 M $AgNO_2$ in the external solution also resulted in deposition of Ag particles. From SEM micrographs of the resulting films, the particles were relatively spherical, uniformly dispersed, and in the size range <0.5 to ~2 μm.

Discussion

Thin films of poly-[Fe(vbpy)$_2$(CN)$_2$],poly-vbpy are capable of providing binding sites for Ag^+ as $AgNO_2$ at one of the cyano groups giving poly-[Fe(vbpy)$_2$(CN)(CNAg)](NO$_2$),poly-vbpy. The failure of both cyano groups to act as ligands is most likely a consequence of the electron-withdrawing effect of the initially bound Ag^+ on the remaining cyano group which decreases its ability to act as an electron donor. There is no direct evidence for binding to free vbpy, but the fact that poly-[Fe(vbpy)$_3$]$^{2+}$ re-forms upon oxidative, reductive, or Ag^+-assisted loss of CN^- shows that it is retained in the films.

From the depth-resolved XPS experiments, it can be concluded that Ag^+ is dispersed throughout the films and is not concentrated at either the electrode–film interface or the film–solution interface. It is translationally labile as shown by its loss when the strongly chelating dithiocarbamide anion is added to the external solution.

Changes in electronic properties and reactivity at Fe^{II} from those of the precursor films are also consistent with cyano binding to Ag^+. This is shown by the shift to higher energies for the Fe^{II} → bpy MLCT bands (Figure 1), the increase in $Fe^{III/II}$ potential, and the Ag^+-assisted labilization of the cyano groups, eq 3. Loss

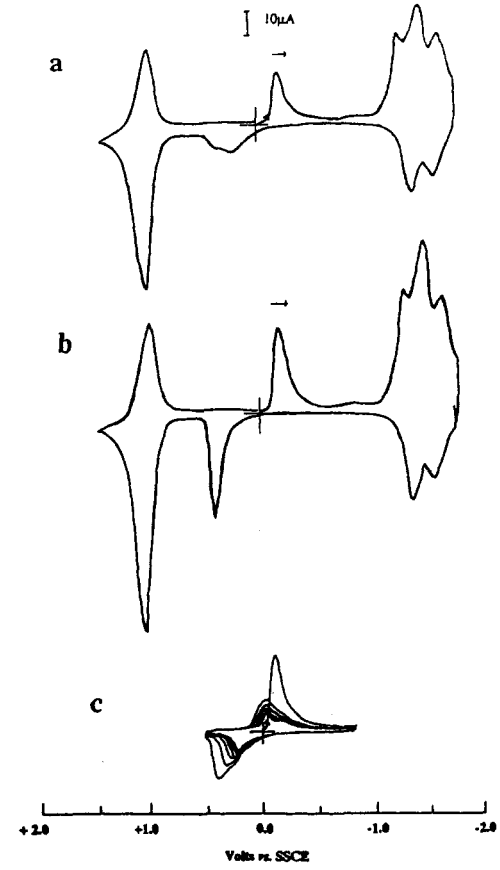

Figure 8. Same as in Figure 4 on poly-$[Fe(vbpy)_3](PF_6)_2{\cdot}2AgNO_2$ at a scan rate of 50 mV/s: (a) a single scan; (b) a single scan after the potential had been held at –1.7 V for 1 min; (c) repetitive scans in the region between –0.8 and +0.5 V following a scan to and potential hold at –0.8 V for 2 min.

of the cyano groups is also induced by oxidation, either by loss of CN^- or formation of cyanogen (eq 4). Loss of CN^- from $M(bpy)_2(CN)_2$ in solution is not facile;[6] in the films, it may be assisted by the neighboring poly-vbpy ligand.

The incorporation of $AgNO_2$ into poly-$[Fe(vbpy)_3](PF_6)_2$ appears to be a partitioning effect dependent on the concentration of $AgNO_2$ in the external solution. The molecular basis for the partitioning is unclear. Given the persistence of the characteristic $\nu(NO_2^-)$ band at 1217 cm^{-1}, there are free NO_2^- anions in these films.

Reduction to Ag^0. Reduction of Ag^+ to Ag^0 occurs in both poly-$[Fe(vbpy)_2(CN)(CNAg)](NO_2)$,poly-vbpy and poly-$[Fe(vbpy)_3](PF_6)_2{\cdot}2AgNO_2$. The fact that the chemical state of Ag^+ is at least slightly different between the two is apparent in the shift to more negative potential for the first scan $Ag^+ \rightarrow Ag^0$ wave which appears at –0.17 for $AgNO_2$ in poly-$[Fe(vbpy)_3](PF_6)_2$ and –0.26 V in the dicyano film.

Following an initial reductive scan in the cyano films, Ag^0 appears to be dispersed throughout, initially still bound to cyanide. The evidence for this is the shift of +0.47 V for the first π^*(vbpy) reduction compared to the Ag-free films. Even at this stage there may be different forms of Ag^0 as evidenced by the complex wave forms for oxidation and reduction. Electron transfer from the electrode must occur by site-to-site, $Ag^0 \rightarrow Ag^+$, electron hopping.

Although Ag^0 may be bound initially to cyanide, at longer times it aggregates to form clusters and colloidal particles. The evidence for this is the appearance of new absorption bands from 350 to 400 nm following reduction at –1.7 V. Reduction for 1 min gave λ_{max} = 380 nm, and reduction for 15 min gave λ_{max} = 400 nm. Similar bands appear following pulse radiolytic reduction of Ag^+ in solutions containing sodium dodecylsulfate.[13] A band appears at 380 nm consistent with colloid formation and an agglomeration number of n = 4 or 6 and particles of radii ≤5 nm. A band 400 nm is consistent with particles of agglomeration number >12 and radii up to 10 nm. This suggests that further aggregation of Ag^0 occurs at longer times in the films.

The spatial distribution of Ag^0 also depends on applied potential and potential hold times. This is illustrated by the time dependence of the wave forms in Figure 5 and the XPS data in Figure 6. With the electrode potential held at –0.7 V, the colloidal particles both aggregate and migrate toward the polymer/electrode interface. From the near match in wave forms for the first oxidative scan after the potential hold in Figure 5a and the stripping wave in Figure 5b, this migration leads to the deposition of Ag^0 at the electrode–film interface. Electrodeposited Ag^0 is removed by oxidative scanning leaving colloidal Ag^0 particles in the bulk. After 12 scans, couples of reduced peak current remain at $E_{p,a}$ = +0.3, +0.2, and –0.1 V.

For poly-$[Fe(vbpy)_3(PF_6)_2{\cdot}2AgNO_2$ reduction of Ag^+ to Ag^0 presumably also occurs by $Ag^+ \rightarrow Ag^0$ reduction, cluster formation, and aggregation to form colloidal particles. With the electrode potential held past –0.7 V, evidence for deposition at the electrode–film interface was also obtained.

A complex $Ag^{+/0}$ redox chemistry exists in these films, and there is a spatial element as well. We have attempted to illustrate below for the cyano films what may occur microscopically at various stages in the electrochemical procedures.

Initial reduction of cyanide-bound Ag^+ to Ag^0 is followed by cluster formation, Ag^0_m, and then formation of colloidal particles, $\{Ag^0\}_n$. From the UV–visible measurements, the size of the particles is $\{Ag^0\}_{4-6}$ at this stage.

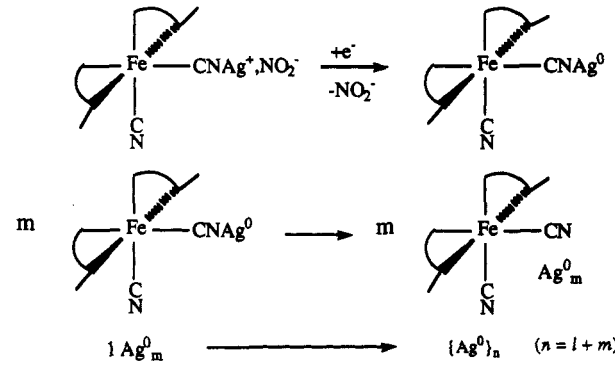

The same final state of aggregation appears to be reached following reduction at –1.7 V (Figure 4c) or at –0.8 V (Figure 5a), i.e. when the potential is held past the initial $Ag^+ \rightarrow Ag^0$ wave at $E_{p,c}$ = –0.26 V. The final pattern of waves after a potential hold and steady-state cycling suggests the presence of at least three discrete redox couples. In steady-state cyclic voltammograms from +0.5 to –0.8 V there are two. The different couples may involve different aggregates or multiple electron transfer in a dominant aggregate. From the chemical reversibility of the waves, the films must provide a well-defined structural basis for maintaining the structural integrity of the $\{Ag^0\}_n/nAg^+$ couples.

Under potential hold conditions, the average particle size increases to $\{Ag^0\}_{>12}$ and the particles migrate to the electrode–film interface, the driving force presumably being the deposition of Ag^0 at the electrode,

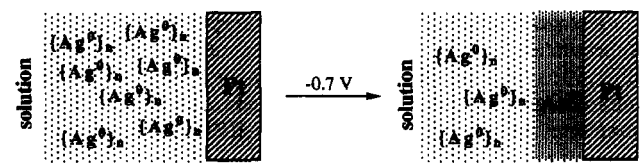

(13) (a) Henglein, A. *J. Am. Chem. Soc.* **1979**, *83*, 2209. (b) Henglein, A.; Tausch-Treml, R. *J. Coll. Inter. Sci.* **1981**, *80*, 84.

Electrodeposited Ag^0 is removed by reoxidation, leaving colloidal particles or clusters dispersed throughout the films which undergo reversible redox cycling indefinitely. The particles or clusters that remain are diluted in the films and stabilized toward further aggregation.

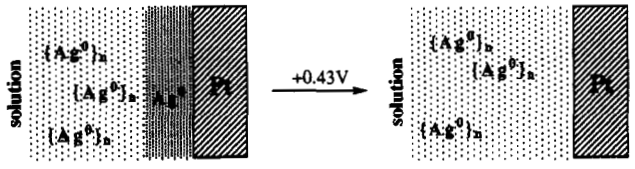

Reduction of Ag^0 impregnated films with $AgNO_2$ in the external solution led to the massive incorporation of Ag^0 with the growth of discrete, <0.5 to 2–3 μm Ag particles on the surface. It is possible that colloidal silver particles at the film–solution interface provide nucleation sites for farther particle growth following $Ag^+ \rightarrow Ag^0$ reduction explaining the discrete, spherical growth pattern.

Acknowledgments are made to the U.S. Army Research Office for Grants DAAL03-88-K-0192 and DAAL03-92-G-0198 in support of this research. We are thankful to Professor Carlo A. Bignozzi for helpful suggestions and to Dr. Mike Mawn for conducting the SEM experiments.